

Fermi National Accelerator Laboratory

FERMILAB-Pub-95/368-E
CDF

**Reconstruction of $B^0 \rightarrow J/\psi K_s^0$ and Measurement of Ratios of
Branching Ratios Involving $B \rightarrow J/\psi K^{(*)}$**

F. Abe et al.

The CDF Collaboration

*Fermi National Accelerator Laboratory
P.O. Box 500, Batavia, Illinois 60510*

November 1995

Submitted to *Physical Review Letters*

Disclaimer

This report was prepared as an account of work sponsored by an agency of the United States Government. Neither the United States Government nor any agency thereof, nor any of their employees, makes any warranty, expressed or implied, or assumes any legal liability or responsibility for the accuracy, completeness, or usefulness of any information, apparatus, product, or process disclosed, or represents that its use would not infringe privately owned rights. Reference herein to any specific commercial product, process, or service by trade name, trademark, manufacturer, or otherwise, does not necessarily constitute or imply its endorsement, recommendation, or favoring by the United States Government or any agency thereof. The views and opinions of authors expressed herein do not necessarily state or reflect those of the United States Government or any agency thereof.

Reconstruction of $B^0 \rightarrow J/\psi K_S^0$ and Measurement of Ratios of Branching Ratios Involving $B \rightarrow J/\psi K^{(*)}$

F. Abe,¹³ M. G. Albrow,⁷ S. R. Amendolia,²² D. Amidei,¹⁶ J. Antos,²⁸ C. Anway-Wiese,⁴ G. Apollinari,²⁶ H. Areti,⁷ M. Atac,⁷ P. Auchincloss,²⁵ F. Azfar,²¹ P. Azzi,²⁰ N. Bacchetta,²⁰ W. Badgett,¹⁶ M. W. Bailey,¹⁸ J. Bao,³⁵ P. de Barbaro,²⁵ A. Barbaro-Galtieri,¹⁴ V. E. Barnes,²⁴ B. A. Barnett,¹² P. Bartalini,²² G. Bauer,¹⁵ T. Baumann,⁹ F. Bedeschi,²² S. Behrends,³ S. Belforte,²² G. Bellettini,²² J. Bellinger,³⁴ D. Benjamin,³¹ J. Benlloch,¹⁵ J. Bensinger,³ D. Benton,²¹ A. Beretvas,⁷ J. P. Berge,⁷ S. Bertolucci,⁸ A. Bhatti,²⁶ K. Biery,¹¹ M. Binkley,⁷ F. Bird,²⁹ D. Bisello,²⁰ R. E. Blair,¹ C. Blocker,³ A. Bodek,²⁵ W. Bokhari,¹⁵ V. Bolognesi,²² D. Bortoletto,²⁴ C. Boswell,¹² T. Boulos,¹⁴ G. Brandenburg,⁹ C. Bromberg,¹⁷ E. Buckley-Geer,⁷ H. S. Budd,²⁵ K. Burkett,¹⁶ G. Busetto,²⁰ A. Byon-Wagner,⁷ K. L. Byrum,¹ J. Cammerata,¹² C. Campagnari,⁷ M. Campbell,¹⁶ A. Caner,⁷ W. Carithers,¹⁴ D. Carlsmith,³⁴ A. Castro,²⁰ Y. Cen,²¹ F. Cervelli,²² H. Y. Chao,²⁸ J. Chapman,¹⁶ M.-T. Cheng,²⁸ G. Chiarelli,²² T. Chikamatsu,³² C. N. Chiou,²⁸ L. Christofek,¹⁰ S. Cihangir,⁷ A. G. Clark,²² M. Cobal,²² M. Contreras,⁵ J. Conway,²⁷ J. Cooper,⁷ M. Cordelli,⁸ C. Couyoumtzelis,²² D. Crane,¹ J. D. Cunningham,³ T. Daniels,¹⁵ F. DeJongh,⁷ S. Delchamps,⁷ S. Dell'Agnello,²² M. Dell'Orso,²² L. Demortier,²⁶ B. Denby,²² M. Deninno,² P. F. Derwent,¹⁶ T. Devlin,²⁷ M. Dickson,²⁵ J. R. Dittmann,⁶ S. Donati,²² R. B. Drucker,¹⁴ A. Dunn,¹⁶ K. Einsweiler,¹⁴ J. E. Elias,⁷ R. Ely,¹⁴ E. Engels, Jr.,²³ S. Eno,⁵ D. Errede,¹⁰ S. Errede,¹⁰ Q. Fan,²⁵ B. Farhat,¹⁵ I. Fiori,² B. Flaughner,⁷ G. W. Foster,⁷ M. Franklin,⁹ M. Frautschi,¹⁸ J. Freeman,⁷ J. Friedman,⁵ A. Fry,²⁹ T. A. Fuess,¹ Y. Fukui,¹³ S. Funaki,³² G. Gagliardi,²² S. Galeotti,²² M. Gallinaro,²⁰ A. F. Garfinkel,²⁴ S. Geer,⁷ D. W. Gerdes,¹⁶ P. Giannetti,²² N. Giokaris,²⁶ P. Giromini,⁸ L. Gladney,²¹ D. Glenzinski,¹² M. Gold,¹⁸ J. Gonzalez,²¹ A. Gordon,⁹ A. T. Goshaw,⁶

K. Goulianos,²⁶ H. Grassmann,⁶ A. Grewal,²¹ L. Groer,²⁷ C. Grosso-Pilcher,⁵ C. Haber,¹⁴
 S. R. Hahn,⁷ R. Hamilton,⁹ R. Handler,³⁴ R. M. Hans,³⁵ K. Hara,³² B. Harral,²¹
 R. M. Harris,⁷ S. A. Hauger,⁶ J. Hauser,⁴ C. Hawk,²⁷ J. Heinrich,²¹ D. Cronin-Hennessy,⁶
 R. Hollebeek,²¹ L. Holloway,¹⁰ A. Hölscher,¹¹ S. Hong,¹⁶ G. Houk,²¹ P. Hu,²³ B. T. Huffman,²³
 R. Hughes,²⁵ P. Hurst,⁹ J. Huston,¹⁷ J. Huth,⁹ J. Hylen,⁷ M. Incagli,²² J. Incandela,⁷
 H. Iso,³² H. Jensen,⁷ C. P. Jessop,⁹ U. Joshi,⁷ R. W. Kadel,¹⁴ E. Kajfasz,^{7a} T. Kamon,³⁰
 T. Kaneko,³² D. A. Kardelis,¹⁰ H. Kasha,³⁵ Y. Kato,¹⁹ L. Keeble,⁸ R. D. Kennedy,²⁷
 R. Kephart,⁷ P. Kesten,¹⁴ D. Kestenbaum,⁹ R. M. Keup,¹⁰ H. Keutelian,⁷ F. Keyvan,⁴
 D. H. Kim,⁷ H. S. Kim,¹¹ S. B. Kim,¹⁶ S. H. Kim,³² Y. K. Kim,¹⁴ L. Kirsch,³
 P. Koehn,²⁵ K. Kondo,³² J. Konigsberg,⁹ S. Kopp,⁵ K. Kordas,¹¹ W. Koska,⁷ E. Kovacs,^{7a}
 W. Kowald,⁶ M. Krasberg,¹⁶ J. Kroll,⁷ M. Kruse,²⁴ S. E. Kuhlmann,¹ E. Kuns,²⁷
 A. T. Laasanen,²⁴ N. Labanca,²² S. Lammel,⁴ J. I. Lamoureux,³ T. LeCompte,¹⁰ S. Leone,²²
 J. D. Lewis,⁷ P. Limon,⁷ M. Lindgren,⁴ T. M. Liss,¹⁰ N. Lockyer,²¹ C. Loomis,²⁷ O. Long,²¹
 M. Loreti,²⁰ E. H. Low,²¹ J. Lu,³⁰ D. Lucchesi,²² C. B. Luchini,¹⁰ P. Lukens,⁷ J. Lys,¹⁴
 P. Maas,³⁴ K. Maeshima,⁷ A. Maghakian,²⁶ P. Maksimovic,¹⁵ M. Mangano,²² J. Mansour,¹⁷
 M. Mariotti,²⁰ J. P. Marriner,⁷ A. Martin,¹⁰ J. A. J. Matthews,¹⁸ R. Mattingly,¹⁵
 P. McIntyre,³⁰ P. Melese,²⁶ A. Menzione,²² E. Meschi,²² G. Michail,⁹ S. Mikamo,¹³ M. Miller,⁵
 R. Miller,¹⁷ T. Mimashi,³² S. Miscetti,⁸ M. Mishina,¹³ H. Mitsushio,³² S. Miyashita,³²
 Y. Morita,³² S. Moulding,²⁶ J. Mueller,²⁷ A. Mukherjee,⁷ T. Muller,⁴ P. Musgrave,¹¹
 L. F. Nakae,²⁹ I. Nakano,³² C. Nelson,⁷ D. Neuberger,⁴ C. Newman-Holmes,⁷ L. Nodulman,¹
 S. Ogawa,³² S. H. Oh,⁶ K. E. Ohl,³⁵ R. Oishi,³² T. Okusawa,¹⁹ C. Pagliarone,²² R. Paoletti,²²
 V. Papadimitriou,³¹ S. P. Pappas,³⁵ S. Park,⁷ J. Patrick,⁷ G. Pauletta,²² M. Paulini,¹⁴
 L. Pescara,²⁰ M. D. Peters,¹⁴ T. J. Phillips,⁶ G. Piacentino,² M. Pillai,²⁵ R. Plunkett,⁷
 L. Pondrom,³⁴ N. Produit,¹⁴ J. Proudfoot,¹ F. Ptohos,⁹ G. Punzi,²² K. Ragan,¹¹ F. Rimondi,²
 L. Ristori,²² M. Roach-Bellino,³³ W. J. Robertson,⁶ T. Rodrigo,⁷ J. Romano,⁵ L. Rosenson,¹⁵
 W. K. Sakumoto,²⁵ D. Saltzberg,⁵ A. Sansoni,⁸ V. Scarpine,³⁰ A. Schindler,¹⁴ P. Schlabach,⁹
 E. E. Schmidt,⁷ M. P. Schmidt,³⁵ O. Schneider,¹⁴ G. F. Sciacca,²² A. Scribano,²² S. Segler,⁷
 S. Seidel,¹⁸ Y. Seiya,³² G. Sganos,¹¹ A. Sgolacchia,² M. Shapiro,¹⁴ N. M. Shaw,²⁴ Q. Shen,²⁴

P. F. Shepard,²³ M. Shimojima,³² M. Shochet,⁵ J. Siegrist,²⁹ A. Sill,³¹ P. Sinervo,¹¹ P. Singh,²³ J. Skarha,¹² K. Sliwa,³³ D. A. Smith,²² F. D. Snider,¹² L. Song,⁷ T. Song,¹⁶ J. Spalding,⁷ L. Spiegel,⁷ P. Sphicas,¹⁵ L. Stanco,²⁰ J. Steele,³⁴ A. Stefanini,²² K. Strahl,¹¹ J. Strait,⁷ D. Stuart,⁷ G. Sullivan,⁵ K. Sumorok,¹⁵ R. L. Swartz, Jr.,¹⁰ T. Takahashi,¹⁹ K. Takikawa,³² F. Tartarelli,²² W. Taylor,¹¹ P. K. Teng,²⁸ Y. Teramoto,¹⁹ S. Tether,¹⁵ D. Theriot,⁷ J. Thomas,²⁹ T. L. Thomas,¹⁸ R. Thun,¹⁶ M. Timko,³³ P. Tipton,²⁵ A. Titov,²⁶ S. Tkaczyk,⁷ K. Tollefson,²⁵ A. Tollestrup,⁷ J. Tonnison,²⁴ J. F. de Troconiz,⁹ J. Tseng,¹² M. Turcotte,²⁹ N. Turini,²² N. Uemura,³² F. Ukegawa,²¹ G. Unal,²¹ S. C. van den Brink,²³ S. Vejcek, III,¹⁶ R. Vidal,⁷ M. Vondracek,¹⁰ D. Vucinic,¹⁵ R. G. Wagner,¹ R. L. Wagner,⁷ N. Wainer,⁷ R. C. Walker,²⁵ C. Wang,⁶ C. H. Wang,²⁸ G. Wang,²² J. Wang,⁵ M. J. Wang,²⁸ Q. F. Wang,²⁶ A. Warburton,¹¹ G. Watts,²⁵ T. Watts,²⁷ R. Webb,³⁰ C. Wei,⁶ C. Wendt,³⁴ H. Wenzel,¹⁴ W. C. Wester, III,⁷ T. Westhusing,¹⁰ A. B. Wicklund,¹ E. Wicklund,⁷ R. Wilkinson,²¹ H. H. Williams,²¹ P. Wilson,⁵ B. L. Winer,²⁵ J. Wolinski,³⁰ D. Y. Wu,¹⁶ X. Wu,²² J. Wyss,²⁰ A. Yagil,⁷ W. Yao,¹⁴ K. Yasuoka,³² Y. Ye,¹¹ G. P. Yeh,⁷ P. Yeh,²⁸ M. Yin,⁶ J. Yoh,⁷ C. Yosef,¹⁷ T. Yoshida,¹⁹ D. Yovanovitch,⁷ I. Yu,³⁵ J. C. Yun,⁷ A. Zanetti,²² F. Zetti,²² L. Zhang,³⁴ S. Zhang,¹⁶ W. Zhang,²¹ and S. Zucchelli²

(CDF Collaboration)

¹ *Argonne National Laboratory, Argonne, Illinois 60439*

² *Istituto Nazionale di Fisica Nucleare, University of Bologna, I-40126 Bologna, Italy*

³ *Brandeis University, Waltham, Massachusetts 02254*

⁴ *University of California at Los Angeles, Los Angeles, California 90024*

⁵ *University of Chicago, Chicago, Illinois 60637*

⁶ *Duke University, Durham, North Carolina 27708*

⁷ *Fermi National Accelerator Laboratory, Batavia, Illinois 60510*

⁸ *Laboratori Nazionali di Frascati, Istituto Nazionale di Fisica Nucleare, I-00044 Frascati, Italy*

⁹ *Harvard University, Cambridge, Massachusetts 02138*

- ¹⁰ *University of Illinois, Urbana, Illinois 61801*
- ¹¹ *Institute of Particle Physics, McGill University, Montreal H3A 2T8, and University of Toronto,
Toronto M5S 1A7, Canada*
- ¹² *The Johns Hopkins University, Baltimore, Maryland 21218*
- ¹³ *National Laboratory for High Energy Physics (KEK), Tsukuba, Ibaraki 305, Japan*
- ¹⁴ *Lawrence Berkeley Laboratory, Berkeley, California 94720*
- ¹⁵ *Massachusetts Institute of Technology, Cambridge, Massachusetts 02139*
- ¹⁶ *University of Michigan, Ann Arbor, Michigan 48109*
- ¹⁷ *Michigan State University, East Lansing, Michigan 48824*
- ¹⁸ *University of New Mexico, Albuquerque, New Mexico 87131*
- ¹⁹ *Osaka City University, Osaka 588, Japan*
- ²⁰ *Universita di Padova, Istituto Nazionale di Fisica Nucleare, Sezione di Padova, I-35131 Padova, Italy*
- ²¹ *University of Pennsylvania, Philadelphia, Pennsylvania 19104*
- ²² *Istituto Nazionale di Fisica Nucleare, University and Scuola Normale Superiore of Pisa, I-56100 Pisa, Italy*
- ²³ *University of Pittsburgh, Pittsburgh, Pennsylvania 15260*
- ²⁴ *Purdue University, West Lafayette, Indiana 47907*
- ²⁵ *University of Rochester, Rochester, New York 14627*
- ²⁶ *Rockefeller University, New York, New York 10021*
- ²⁷ *Rutgers University, Piscataway, New Jersey 08854*
- ²⁸ *Academia Sinica, Taiwan 11529, Republic of China*
- ²⁹ *Superconducting Super Collider Laboratory, Dallas, Texas 75237*
- ³⁰ *Texas A&M University, College Station, Texas 77843*
- ³¹ *Texas Tech University, Lubbock, Texas 79409*
- ³² *University of Tsukuba, Tsukuba, Ibaraki 305, Japan*
- ³³ *Tufts University, Medford, Massachusetts 02155*
- ³⁴ *University of Wisconsin, Madison, Wisconsin 53706*
- ³⁵ *Yale University, New Haven, Connecticut 06511*

We report on the reconstruction of the decay mode $B^0 \rightarrow J/\psi K_S^0$ using 19.3 pb⁻¹ of data collected by the Collider Detector at Fermilab in $\bar{p}p$ collisions at $\sqrt{s} = 1.8$ TeV. A signal of 41.8 ± 6.9 events, with a signal-to-background ratio of 9:1, is observed. Three additional decay modes $B^+ \rightarrow J/\psi K^+$, $B^0 \rightarrow J/\psi K^*(892)^0$ and $B^+ \rightarrow J/\psi K^*(892)^+$ are reconstructed. We measure three ratios of branching ratios, each one relative to the $B^+ \rightarrow J/\psi K^+$ mode. We also report the ratio of production rates, $\Gamma(B \rightarrow J/\psi K^*)/\Gamma(B \rightarrow J/\psi K)$, for the vector-vector relative to the vector-pseudoscalar modes, to be 1.32 ± 0.23 (stat.) ± 0.16 (syst.).

PACS numbers: 13.25.Hw, 14.40.Nd

PACS numbers: 13.25.Hw, 14.40.Nd

This Letter reports on the reconstruction of the decay $B^0 \rightarrow J/\psi K_S^0$ [1] with the subsequent decay $K_S^0 \rightarrow \pi^+\pi^-$ and on three additional $B \rightarrow J/\psi K^{(*)}$ modes [2]. We reconstruct the isospin partner $B^+ \rightarrow J/\psi K^+$ and the pseudoscalar-to-vector-vector transitions, $B^0 \rightarrow J/\psi K^*(892)^0$ and $B^+ \rightarrow J/\psi K^*(892)^+$. We measure three ratios of branching ratios: $BR(B^0 \rightarrow J/\psi K^0)/BR(B^+ \rightarrow J/\psi K^+)$, $BR(B^0 \rightarrow J/\psi K^*(892)^0)/BR(B^+ \rightarrow J/\psi K^+)$, $BR(B^+ \rightarrow J/\psi K^*(892)^+)/BR(B^+ \rightarrow J/\psi K^+)$, and report the ratio formed by combining the pseudoscalar-to-vector-vector modes relative to the pseudoscalar-to-vector-pseudoscalar modes, which we refer to as the “vector-pseudoscalar ratio”. By forming ratios, we minimize several systematic uncertainties, the largest of which are associated with the b -quark production cross section and transverse momentum spectrum. Together with information on the polarization in the decay $B \rightarrow J/\psi K^*$ [3–5], these decay modes are of particular interest to test theoretical predictions that depend on the factorization hypothesis [6,7] and the $B \rightarrow K^{(*)}$ form factor [8].

The decay mode $B^0 \rightarrow J/\psi K_S^0$ is expected to provide the first observation of CP violation outside the kaon system. From a theoretical point of view, the decay $B^0 \rightarrow J/\psi K_S^0$

has several properties that make it ideal for the search for CP violation in the b -quark system [9,10]. Experimentally, a large cross section for B meson production at the Tevatron collider has been measured [11]. Furthermore, the decay of the $J/\psi \rightarrow \mu^+\mu^-$ simplifies the triggering and the long lifetime of the K_S^0 permits the isolation of a clean K_S^0 signal in the hadron collider environment without explicit particle identification.

The data used in this analysis were collected with the Collider Detector at Fermilab (CDF) during the 1992-1993 run. The data correspond to an integrated luminosity of 19.3 pb⁻¹ of $\bar{p}p$ collisions at $\sqrt{s} = 1.8$ TeV. The CDF detector is described in detail elsewhere [12]. We describe here only the detector components most relevant to this analysis. Two devices inside the 1.4 T solenoid are used for the tracking of charged particles: the silicon vertex detector (SVX) and the central tracking chamber (CTC). The SVX consists of four layers of silicon microstrip detectors located at radii between 3.0 and 7.9 cm from the interaction point and provides spatial measurements in the r - φ plane [13], giving a track impact parameter resolution of $(13 + 40/P_T)$ μm [14], where P_T is the transverse momentum of the track in GeV/ c . The CTC is a cylindrical drift chamber containing 84 layers grouped into nine alternating superlayers of axial and stereo wires. It covers the pseudorapidity interval $|\eta| < 1.1$, where $\eta = -\ln[\tan(\theta/2)]$. The P_T resolution of the CTC combined with the SVX is $\delta(P_T)/P_T = ((0.0066)^2 + (0.0009P_T)^2)^{1/2}$. Two muon subsystems in the central region were used, the central muon chambers and the central muon extension, which together provide coverage in the interval $|\eta| < 1.0$.

Dimuon events were collected using a three-level trigger system. The first level required two charged tracks in the muon chambers. The efficiency for finding a muon at level one rises from 30% at $P_T = 1.5$ GeV/ c to 93% for $P_T > 3$ GeV/ c . Level two requires that at least one of the muon tracks match a charged track in the CTC found with the Central Fast Track (CFT) processor. The efficiency for finding a CTC track in the CFT at level two rises from 50% for $P_T > 2.6$ GeV/ c to 94% for $P_T > 3.1$ GeV/ c . The third level software trigger requires that two oppositely charged CTC tracks each match muon track segments and that the $\mu^+\mu^-$ invariant mass is between 2.8 and 3.4 GeV/ c^2 to select J/ψ candidates.

The B meson reconstruction starts with the isolation of the J/ψ signal. First, the CTC track is extrapolated to the muon chambers and this position is required to match the muon track segment to within three standard deviations, which is derived from the multiple scattering and measurement errors. Only tracks measured in three dimensions by the CTC are used and good quality SVX information is added when available, which is in approximately 50% of the candidates. We calculate the invariant mass of two oppositely charged muon candidates after constraining them to originate from a common point in space (“vertex constraint”). The confidence level (CL) of the fit is required to be greater than 1%. We require one muon with $P_T > 1.8$ GeV/ c and the other one with $P_T > 2.5$ GeV/ c to ensure we operate in a well-measured region of the trigger efficiency. We find 62146 ± 299 J/ψ meson candidates with a signal-to-background ratio of 5:1 [15].

After mass constraining the J/ψ to the world average value [16] and requiring the CL > 1%, the next step is to search for kaon candidates from all other tracks within the CTC fiducial volume. For the $J/\psi K^+$ mode, every track is considered a kaon candidate. The K_S^0 selection requires two oppositely charged tracks with $P_T > 0.35$ GeV/ c , each track satisfying $d_\pi/\sigma_{d_\pi} > 2$, where d_π is the distance of closest approach to the beam position, and σ_{d_π} is the corresponding uncertainty, which includes the track measurement errors and the beam position uncertainty. The $\pi^+\pi^-$ pairs are vertex constrained, required to point to the J/ψ vertex and satisfy the requirement, CL > 1%. A signed two-dimensional decay length $L_{xy}(K_S^0)$, defined as the displacement of the K_S^0 vertex projected onto the direction of the $P_T(K_S^0)$, is required to be greater than 1.0 cm. We find 7733 ± 101 K_S^0 candidates with a signal-to-background ratio of 7:1 [15]. The $K^*(892)^+$ candidate is formed with a K_S^0 candidate plus a track, assumed to be a π^+ , and the $K^*(892)^0$ candidate is formed from two charged tracks assumed to be a K^+ and a π^- . The K - π particle assignment with invariant mass closest to the world average mass [16] of the $K^*(892)^0$ is retained and combinations where the K^* mass is greater than 75 MeV/ c^2 from the world average mass are rejected.

Several constraints are imposed to improve the B mass resolution. In order to maximize the combinatoric background rejection, these constraints are applied incrementally and for

each added constraint we require $\text{CL}(\Delta\chi^2) > 1\%$, where $\Delta\chi^2$ is the change in χ^2 due to the additional constraint. For the $J/\psi K^+$ mode, the K^+ candidate track is added to the J/ψ vertex constraint. For the $J/\psi K_S^0$ mode, K_S^0 decay products are vertex and mass constrained and the K_S^0 is constrained to point to the J/ψ vertex in three dimensions. For the $J/\psi K^*(892)^+$ mode, the K_S^0 is constrained to point to the three-track $J/\psi\pi^+$ vertex and for the $J/\psi K^*(892)^0$ mode, the four tracks are vertex constrained. For all four modes, the B candidate system is constrained to point to the primary vertex.

To further reduce the combinatoric background, we require $P_T(K^{(*)}) > 1.5 \text{ GeV}/c$, $P_T(B) > 7 \text{ GeV}/c$, and $c\tau(B) > 100 \text{ }\mu\text{m}$, where $c\tau(B)$ is computed using the displacement of the J/ψ vertex projected onto the direction of the $P_T(B)$. The normalized mass distributions are shown in Fig. 1 for $J/\psi K^+$, $J/\psi K_S^0$, and in Fig. 2 for the $J/\psi K^*(892)^0$ and $J/\psi K^*(892)^+$. The normalized mass is computed for each candidate by dividing the difference between the invariant mass and the world average B mass [16] by the error on the mass, where the error is determined using the full covariance matrix for each candidate. The normalized mass follows a Gaussian shape more closely than the invariant mass distribution. The number of signal events is obtained by fitting a Gaussian of width fixed to 1.0 and a flat background to the normalized mass distributions. The binned maximum likelihood method gives 169 ± 18 , 41.8 ± 6.9 , 71 ± 12 , and 17.0 ± 4.7 signal events in the $B^+ \rightarrow J/\psi K^+$, $B^0 \rightarrow J/\psi K_S^0$, $B^0 \rightarrow J/\psi K^*(892)^0$, and $B^+ \rightarrow J/\psi K^*(892)^+$ channels, respectively. The signal-to-background ratios [15] are given in Table I.

The ratio of branching ratios is computed using the relation:

$$\frac{BR(B^0 \rightarrow J/\psi K^0)}{BR(B^+ \rightarrow J/\psi K^+)} = \frac{2N(J/\psi K_S^0)}{N(J/\psi K^+)} \times \frac{\epsilon_{J/\psi K^+}}{\epsilon_{J/\psi K_S^0}} \times \frac{1}{BR(K_S^0 \rightarrow \pi^+ \pi^-)},$$

where the factor of two corrects for $K^0 \rightarrow K_L^0$, which is not reconstructed, and we assume equal production rates of B^+ and B^0 mesons. World average branching ratios are used for all $K^{(*)}$ daughter decays [16], an isospin analysis determines $BR(K^*(892)^0 \rightarrow K^+ \pi^-) = 2/3$ and $BR(K^*(892)^+ \rightarrow K^0 \pi^+) = 2/3$.

The reconstruction efficiencies are factorized as:

$$\epsilon_{J/\psi K^+} = \epsilon_{P_T(B)} \times \epsilon_{c\tau(B)} \times \epsilon_{J/\psi} \times \epsilon_{P_T(K^+)} \times \epsilon_{J/\psi K^+}^R$$

$$\epsilon_{J/\psi K_S^0} = \epsilon_{P_T(B)} \times \epsilon_{c\tau(B)} \times \epsilon_{J/\psi} \times \epsilon_{P_T(K_S^0)} \times \epsilon_{J/\psi K_S^0}^R.$$

The efficiency of the $P_T(B)$ cut ($\epsilon_{P_T(B)}$), the $c\tau(B)$ cut ($\epsilon_{c\tau(B)}$), the $P_T(K)$ cut ($\epsilon_{P_T(K)}$), and the efficiency for finding the J/ψ ($\epsilon_{J/\psi}$), all cancel in the ratio. However, some of the efficiencies associated with the K_S^0 decay do not cancel in the ratio. The superscript R denotes the remaining terms. To further facilitate cancellation, these terms are factorized as:

$$\epsilon_{J/\psi K^+}^R = \epsilon_{K^+}^G \times \epsilon_{\text{Trk}(K^+)} \times \epsilon_{\Delta\chi^2(J/\psi K^+)}$$

$$\epsilon_{\Delta\chi^2(J/\psi K^+)} = \epsilon_{V(\mu^+\mu^-)} \times \epsilon_{M(\mu^+\mu^-)} \times \epsilon_{V(K^+)} \times \epsilon_{P_{xy}(J/\psi K^+)} \times \epsilon_{P_z(J/\psi K^+)}$$

and

$$\epsilon_{J/\psi K_S^0}^R = \epsilon_{K_S^0} \times \epsilon_{\Delta\chi^2(J/\psi K_S^0)}$$

$$\epsilon_{K_S^0} = \epsilon_{\pi}^G \times \epsilon_{P_T(\pi)} \times \epsilon_{\text{Trk}(K_S^0)} \times \epsilon_{L_{xy}} \times \epsilon_{d\pi}$$

$$\epsilon_{\Delta\chi^2(J/\psi K_S^0)} = \epsilon_{V(\mu^+\mu^-)} \times \epsilon_{M(\mu^+\mu^-)} \times \epsilon_{V(\pi^+\pi^-)} \times \epsilon_{P(\pi^+\pi^-)} \times \epsilon_{M(\pi^+\pi^-)} \times \epsilon_{P_{xy}(J/\psi K_S^0)} \times \epsilon_{P_z(J/\psi K_S^0)}$$

where the superscript G indicates the term is a geometrical acceptance, V , M , and P indicate a vertex, mass, or pointing constraint, respectively, while P_{xy} and P_z refer to pointing constraints in the x - y plane and z direction. We cancel the $\epsilon_{V(K^+)}$ against the $\epsilon_{P(\pi^+\pi^-)}$ term and have verified the cancellation by Monte Carlo simulation. Canceling the remaining terms in the expansion of $\epsilon_{\Delta\chi^2(J/\psi K^+)}$ against similar terms in $\epsilon_{\Delta\chi^2(J/\psi K_S^0)}$, leaves the efficiency product $\epsilon_{\Delta\chi^2(J/\psi K_S^0)}^R = \epsilon_{V(\pi^+\pi^-)} \times \epsilon_{M(\pi^+\pi^-)}$.

The geometrical acceptances, the $\epsilon_{P_T(\pi)}$ term, the tracking efficiencies (ϵ_{Trk}), and the $\epsilon_{L_{xy}}$ are calculated using a Monte Carlo simulation that incorporates the following:

- (1) The b -quark P_T and rapidity distributions follow the next-to-leading order QCD [17] calculation with MRS D0 [18] proton structure functions. We generate b quarks with rapidity $|y| < 1.0$.

(2) The $B^+ \rightarrow J/\psi K^+$ and the $B^0 \rightarrow J/\psi K^0$ decays involve a pseudoscalar-to-vector-pseudoscalar decay. In the J/ψ rest frame, the decay muons follow a $\sin^2 \theta$ angular distribution with respect to the kaon direction in the rest frame of the B meson.

(3) We measure the efficiency of the CTC track reconstruction algorithm by embedding simulated tracks in real data J/ψ events. The tracks are generated so as to permit the reconstruction of the B mass [2]. The kaons are required to have $P_T > 1.5$ GeV/ c . Only tracks within the CTC fiducial volume are embedded. We measure a tracking efficiency of $\epsilon_{\text{Trk}(K^+)} = (92.0 \pm 2.0 \text{ (syst.)})\%$ for K^+ . This result includes the effect of the K^+ finite lifetime. The K_S^0 tracking efficiency is $\epsilon_{\text{Trk}(K_S^0)} = (86.0 \pm 2.0 \text{ (syst.)})\%$ for $P_T(\pi) > 0.35$ GeV/ c .

The efficiency of the $d_\pi/\sigma_{d_\pi} > 2$ cut (ϵ_{d_π}), and the efficiencies of the $\text{CL}(\Delta\chi^2) > 1\%$ requirement on the vertex and mass constraints of the $\pi^+\pi^-$ pairs ($\epsilon_{V(\pi^+\pi^-)}$, $\epsilon_{M(\pi^+\pi^-)}$), were obtained from the inclusive K_S^0 sample. In summary we determine the ratio of efficiencies to be $\epsilon_{J/\psi K^+}/\epsilon_{J/\psi K_S^0} = 1.57 \pm 0.08 \text{ (syst.)}$.

For the $J/\psi K^*(892)^0$ and the $J/\psi K^*(892)^+$ decay modes, the efficiencies are factorized in the same manner. For both ratios, $J/\psi K^*(892)^0/J/\psi K^+$ and $J/\psi K^*(892)^+/J/\psi K^+$, the efficiencies for the cuts on $c\tau(B)$ and $P_T(B)$, will cancel.

The efficiency for finding the J/ψ and the efficiency of the $P_T(K^{(*)})$ cut do not completely cancel because of the K^* polarization and the K^*-K mass difference. Both of these ratios are corrected for the acceptance of the K^* mass window, which is computed by integrating a Breit-Wigner distribution.

Each $J/\psi K^*/J/\psi K^+$ ratio also has unique non-canceling efficiencies. For the $K^*(892)^0$ case, there is the effect of slightly different geometrical acceptances and efficiencies for the K^+ , as well as four terms associated with the π^- : the efficiency of the $P_T(\pi)$ cut, the track and geometric efficiencies, and the efficiency of adding an extra track to the vertex constraint.

For the $J/\psi K^*(892)^+/J/\psi K^+$ ratio, both modes have a charged track originating from the B decay vertex. However, the geometric acceptance, track reconstruction, kinematic and

$\text{CL}(\Delta\chi^2)$ cut efficiencies are slightly different. The efficiencies associated with the K_S^0 do not cancel, and are determined in the same manner outlined previously. We use the Monte Carlo method described above to compute the ratio of the remaining efficiencies. The efficiencies and numbers of events for all four modes are summarized in Table I.

Six sources of systematic uncertainty contribute to the ratio of efficiencies. Each uncertainty in the lifetimes, τ_{B^+} and τ_{B^0} , contributes a 2% uncertainty to the $c\tau(B) > 100 \mu\text{m}$ cut. This contributes a 2.8% systematic error for the ratio of efficiencies. The ratio of tracking efficiencies has a 2–3.5% systematic error, depending on the mode. The $\text{CL}(\Delta\chi^2) > 1\%$ requirement adds 2–2.8% and was determined from the inclusive K_S^0 sample. Polarization, (Γ_L/Γ) , uncertainties contribute 1.9–2.4% and the variation of the b -quark P_T spectrum in the Monte Carlo simulation contribute 1.7–7.6%. In the two cases where the J/ψ trigger efficiencies do not cancel due to different polarization effects in the ratio, we determine the ratio of the number of events with and without a trigger requirement, and assign an additional 5% uncertainty due to the difference in the ratios. The uncertainties are combined in quadrature, and are summarized in Table II.

We find the ratios of branching ratios to be:

$$BR(B^0 \rightarrow J/\psi K^0)/BR(B^+ \rightarrow J/\psi K^+) = 1.13 \pm 0.22 \text{ (stat.)} \pm 0.06 \text{ (syst.)}$$

$$BR(B^0 \rightarrow J/\psi K^*(892)^0)/BR(B^+ \rightarrow J/\psi K^+) = 1.33 \pm 0.27 \text{ (stat.)} \pm 0.11 \text{ (syst.)}$$

$$BR(B^+ \rightarrow J/\psi K^*(892)^+)/BR(B^+ \rightarrow J/\psi K^+) = 1.55 \pm 0.46 \text{ (stat.)} \pm 0.16 \text{ (syst.)}.$$

We also determine the combined vector-to-pseudoscalar ratio using all four modes to be

$$R = \Gamma(B \rightarrow J/\psi K^*)/\Gamma(B \rightarrow J/\psi K) = 1.32 \pm 0.23 \text{ (stat.)} \pm 0.16 \text{ (syst.)},$$

where we assume equal production of B^+ and B^0 mesons and the systematic error is summarized in Table II. The dominant systematic uncertainty of 9% comes from the B meson lifetime ratio, τ_{B^+}/τ_{B^0} [16]. In addition we use the world average value $BR(B^+ \rightarrow J/\psi K^+) = (1.02 \pm 0.14) \times 10^{-3}$ [16] to obtain three branching ratios

$$BR(B^0 \rightarrow J/\psi K^0) = [1.15 \pm 0.23 \text{ (stat.)} \pm 0.17 \text{ (syst.)}] \times 10^{-3}$$

$$BR(B^0 \rightarrow J/\psi K^*(892)^0) = [1.36 \pm 0.27 \text{ (stat.)} \pm 0.22 \text{ (syst.)}] \times 10^{-3}$$

$$BR(B^+ \rightarrow J/\psi K^*(892)^+) = [1.58 \pm 0.47 \text{ (stat.)} \pm 0.27 \text{ (syst.)}] \times 10^{-3},$$

where the quoted systematic error includes the uncertainty in the $BR(B^+ \rightarrow J/\psi K^+)$. These results are consistent with the current world average values [16].

In conclusion, we have presented the details of the reconstruction of the CP eigenstate $B^0 \rightarrow J/\psi K_S^0$ in a hadron collider environment and demonstrated that a good signal-to-background ratio is achieved. We have reported three branching ratios using $B^0 \rightarrow J/\psi K^*(892)^0$, $B^+ \rightarrow J/\psi K^*(892)^+$, and $B^0 \rightarrow J/\psi K^0$ relative to $B^+ \rightarrow J/\psi K^+$, which are comparable in precision and in good agreement with the current world average values [16].

We also combine these four decay modes to determine the vector-to-pseudoscalar ratio and confirm a previous determination of $R = 1.64 \pm 0.34$ [19], where naive spin counting would predict a value of three for the vector-to-pseudoscalar ratio. Theoretical models [6–8] that assume the factorization hypothesis and use current meson form factors are presently not able to simultaneously accommodate a low vector-to-pseudoscalar ratio and the polarization data [5]. This measurement reinforces the need for a better understanding of these models.

We thank the Fermilab staff and the staffs of the participating institutions for their vital contributions. This work was supported by the U.S. Department of Energy and National Science Foundation; the Italian Istituto Nazionale di Fisica Nucleare; the Ministry of Education, Science and Culture of Japan; the Natural Sciences and Engineering Research Council of Canada; the National Science Council of the Republic of China; the A. P. Sloan Foundation; and the Alexander von Humboldt-Stiftung.

[1] References to a specific state imply the charge-conjugate state as well.

[2] J. Gonzalez-Atavales, Ph.D. thesis, University of Pennsylvania, 1995.

- [3] H. Albrecht *et al.*, Phys. Lett. B **340**, 217 (1994).
- [4] M. S. Alam *et al.*, Phys. Rev. D **50**, 43 (1994).
- [5] F. Abe *et al.*, Phys. Rev. Lett. **75**, 3068 (1995).
- [6] M. Wirbel, B. Stech, and M. Bauer, Z. Phys. C**29**, 637 (1985); M. Bauer, B. Stech, and M. Wirbel, Z. Phys. C**34**, 103 (1987).
- [7] M. Gourdin, A. N. Kamal, and X. Y. Pham, Phys. Rev. Lett. **73**, 3355 (1994).
- [8] R. Aleksan *et al.*, Phys. Rev. D **51**, 6235 (1995).
- [9] For a review see *B Decays*, edited by S. Stone, 2nd ed. (World Scientific, Singapore, 1994).
- [10] I.I. Bigi and A.I. Sanda, Nucl. Phys. B**193**, 85 (1981); I. Dunietz, in *B Decays*, Ref. [9]; Y. Nir and H. Quinn, in *B Decays*, Ref. [9].
- [11] F. Abe *et al.*, Phys. Rev. Lett. **75**, 1451 (1995).
- [12] F. Abe *et al.*, Nucl. Instrum. Methods Phys. Res., Sect. A **271**, 387 (1988).
- [13] In CDF, φ is the azimuthal angle, θ is the polar angle measured from the proton direction, and r is the radius from the beam axis (z -axis).
- [14] D. Amidei *et al.*, Nucl. Instrum. Methods Phys. Res., Sect. A **350**, 73 (1994).
- [15] The background is computed in a $\pm 2.5\sigma$ region around the peak. In the case of the J/ψ and K_S^0 signals, we fit a double Gaussian and use the larger width as σ .
- [16] *Particle Data Group*, L. Montanet *et al.*, Phys. Rev. D **50** (1994).
- [17] S. Dawson *et al.*, Nucl. Phys. B **327**, 49 (1988); M. Mangano *et al.*, Nucl. Phys. B **373**, 295 (1992).
- [18] A. D. Martin, W. J. Stirling, and R.G. Roberts, Phys. Rev. D **47**, 867 (1993).
- [19] T.E. Browder, K. Honscheid, and S. Playfer, *B Decays*, Ref. [9].

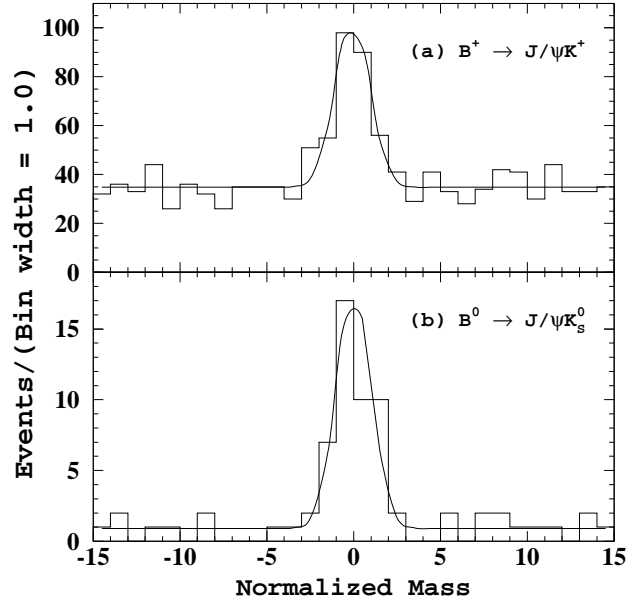


FIG. 1.

The normalized mass distribution for (a) $J/\psi K^+$ and (b) $J/\psi K_S^0$ after all cuts.

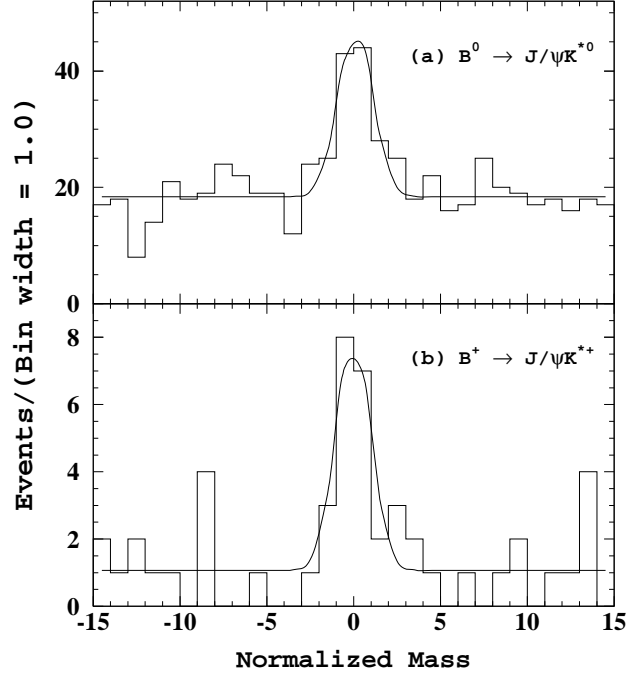


FIG. 2.

The normalized mass distribution for (a) $J/\psi K^{*}(892)^0$ and (b) $J/\psi K^{*}(892)^+$ after all cuts.

TABLE I. Summary of number of events, signal-to-background (S/B), and ratios of efficiencies relative to the $B^+ \rightarrow J/\psi K^+$ decay mode.

	$J/\psi K^+$	$J/\psi K_S^0$	$J/\psi K^*(892)^0$	$J/\psi K^*(892)^+$
Number of Events	169 ± 18	41.8 ± 6.9	71 ± 12	17.0 ± 4.7
S/B	0.97	9.23	0.77	3.12
Ratio of efficiencies	-	1.57 ± 0.08	2.11 ± 0.18	3.53 ± 0.37

TABLE II. Summary of systematic uncertainties (%) for the ratios of branching ratios.

	$\epsilon_{J/\psi K^+} / \epsilon_{J/\psi K_S^0}$	$\epsilon_{J/\psi K^+} / \epsilon_{J/\psi K^{*0}}$	$\epsilon_{J/\psi K^+} / \epsilon_{J/\psi K^{*+}}$	ϵ_V / ϵ_P
τ_{B^+} / τ_{B^0}	2.8	2.8	-	9
Trk Efficiency	2.8	2	3.5	2.1
$\text{CL}(\Delta\chi^2)$	2.8	2	3.5	2.1
Γ_L / Γ	-	1.9	2.4	1.9
$P_T(b)$ Variations	1.7	5.4	7.6	5.5
Trigger	-	5	5	5
Total	5.0%	8.6%	10.6%	12%